Am J Nucl Med Mol Imaging 2023;13(4):171-178
www.ajnmmi.us /ISSN:2160-8407/ajnmmi0152137

Original Article

Automated radiosynthesis of [^{18}F]FMPEP-d_2 for cannabinoid receptor PET imaging

Huailei Jiang[1,2,3], Yan Guo[1,2,3], Otto Muzik[2,4]

[1]Cyclotron and Radiochemistry Core, Karmanos Cancer Institute, Detroit, MI, USA; [2]PET Center, Karmanos Cancer Institute, Detroit, MI, USA; [3]Department of Oncology, Wayne State University, Detroit, MI, USA; [4]Department of Pediatrics and Neurology, Wayne State University, Detroit, MI, USA

Received July 10, 2023; Accepted July 20, 2023; Epub August 15, 2023; Published August 30, 2023

Abstract: The cannabinoid subtype 1 receptor (CB1R) is highly expressed in the central nervous system and abnormalities in regional CB1R density are associated with neurodegenerative disorders. The PET tracer [^{18}F]FMPEP-d_2 is an inverse CB1R agonist which was shown to be suitable for non-invasive PET imaging. In this work, we reported the fully automated radiosynthesis of [^{18}F]FMPEP-d_2 on a Synthra RNplus research module. In a total synthesis time of 70 min, [^{18}F]FMPEP-d_2 was obtained in 2.2 ± 0.1 GBq (n = 3) with excellent radiochemical and chemical purity. Quality control test showed that [^{18}F]FMPEP-d_2 product meets all the release criteria for clinical patient use.

Keywords: Cannabinoid receptor, [^{18}F]FMPEP-d_2, radiosynthesis, automation, PET imaging, radiopharmaceutical

Introduction

Cannabinoid subtype 1 receptor (CB1R) is a neuromodulator highly expressed in the central nervous system [1, 2] and coupled to memory, learning and addiction processes [3, 4]. Moreover, changes in brain CB1R distribution have been shown to be associated with a variety of neurodegenerative disorders such as Huntington's disease, schizophrenia and Alzheimer's disease [5, 6]. Positron emission tomography (PET) provides an important tool for non-invasive imaging of central nervous system related diseases [7-9], and CB1R has been investigated as a target to understand the molecular mechanisms underlying these neurodegenerative disorders.

The ideal CB1R radiotracers should have low non-specific bindings, high CB1R affinity and be able to cross blood-brain barrier (BBB). The first-generation CB1R radiotracers, such as (-)-5'-[^{18}F]fluoro-Δ^8-THC [10] and [^{18}F]AM5144 [11], were limited by their non-specific binding and poor BBB permeability. Following that, more second-generation CB1R radiotracers were developed with reduced lipophilicity and higher affinity. Among them (**Figure 1**), [^{18}F]FMPEP-d_2 was designed based on its [^{11}C]MePPEP analog with suitable lipophilicity and specific CB1R binding [12]. Therefore, [^{18}F]FMPEP-d_2 was extensively investigated as a tool for PET imaging of CB1R related applications, such as neurological disorders [13], and brown adipose tissue [14], alcohol abuse [15].

The radiosynthesis of [^{18}F]FMPEP-d_2 was originally reported by Donohue et al. [12], with the reaction of (3R,5R)-5-(3-hydroxyphenyl)-3-[(R)-1-phenylethylamino]-1-(4-trifluoromethylphenyl) pyrrolidine-2-one (PPEP precursor) and [^{18}F]bromofluoromethane-d_2 ([^{18}F]FCD$_2$Br), which is a volatile intermediate formed by radiofluorination of dibromomethane-d_2 (CD$_2$Br$_2$) with azeotropically dried [^{18}F]fluoride and kryptofix 2.2.2 mixture (**Figure 2**). Lahdenpohja et al. [16] reported an improved [^{18}F]FMPEP-d_2 synthesis on an in-house built module but requiring additional gas chromatography for [^{18}F]FCD$_2$Br separation. To meet the needs of in-human PET imaging, there are demands for the development of automated [^{18}F]FMPEP-d_2 production on commercially available synthesizers. Synthra RNplus research module is one of the synthesizers for advanced radiotracers production [17-19]. In this work, we report the fully automated radiosynthesis of [^{18}F]FMPEP-d_2 on RNplus research module with slight modification of

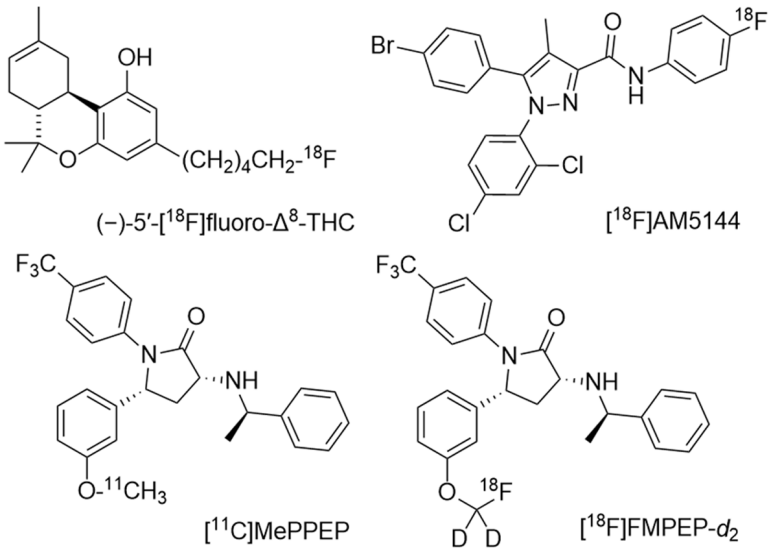

Figure 1. Representative chemical structures of CB1R-targeting PET tracers.

Donohue et al.'s method [12], and its quality control following good manufacturing practices (GMP).

Materials and methods

General

Unless otherwise stated, reagents, solvents, and chemicals were purchased from commercially available vendors and used without further purification. The (3R,5R)-5-(3-hydroxyphenyl)-3-[(R)-1-phenylethylamino]-1-(4-trifluoromethylphenyl)pyrrolidine-2-one (PPEP) precursor and [^{19}F]FMPEP reference standard compound were purchased from PharmaSynth AS (Tartu, Estonia). Acetonitrile (MeCN; anhydrous 99.8%), N,N-dimethylformamide (DMF; anhydrous 99.8%), potassium carbonate (K_2CO_3; 99.995% trace metals basis), cesium carbonate (Cs_2CO_3; 99.9% trace metals basis), dibromomethane-d_2 (CD_2Br_2; 99 atom% D with copper stabilizer), 1,4,7,10,13,16-hexaoxacyclooctadecane (18-crown-6; ≥ 99.0%), trifluoroacetic acid (TFA; > 99.0%), and 0.22 μm PTFE Millex-LG syringe filter unit (33 mm) were purchased from Millipore Sigma (St. Louis, MO, USA). Acetonitrile (MeCN; HPLC grade) was purchased from Fisher Scientific (Hampton, NH, USA). Kryptofix 2.2.2 ($K_{2.2.2}$; chemical grade) and [^{18}O]H_2O (≥ 98%) was purchased from ABX (Radeberg, Germany). QMA carbonate plus light cartridge (46 mg sorbent per cartridge; 40 μm), silica plus cartridge (690 mg sorbent per cartridge; 55-105 μm), and C18 plus short cartridge (400 mg sorbent per cartridge; 37-55 μm) were purchased from Waters (Milford, MA, USA). Absolute ethanol (EtOH; USP grade) was purchased from Greenfield Global USA Inc. (Shelbyville, KY, USA). Sterile water for injection, USP and 0.9% sodium chloride (NaCl) for injection, USP were purchased from Hospira (Lake Forest, IL, USA). Fresh deionized water (18.2 MΩ·cm at 25°C) was generated from Milli-Q Direct water purification system (Millipore Sigma, Billerica, MA, USA), and used for the preparation of all the standard and eluent solutions. The $K_{2.2.2}/K_2CO_3$ stock solution for [^{18}F]fluoride elution was prepared with $K_{2.2.2}$ (240 mg) and K_2CO_3 (40 mg) in acetonitrile (19.4 mL) and deionized water (0.6 mL), and passed through a Millex-LG PTFE filter (Millipore Sigma, St. Louis, MO, USA). Prior to use, QMA cartridge was conditioned with 5 mL deionized water, and C18 cartridge was conditioned with 5 mL ethanol and 5 mL deionized water. Radioactivity was determined with a Capintec® CRC-712M dose calibrator (Capintec, Inc., Florham Park, NJ, USA).

Chromatographic method

Semi-preparative high-performance liquid chromatography (HPLC) was carried out on an RNplus Research module (Synthra, Hamburg, Germany), which included a built-in semi-preparative HPLC system with ultraviolet (UV) and radioactivity detectors. [^{18}F]FMPEP-d_2 purification was conducted on a Nucleodur Pyramid C18 column (5 μm, 10 × 250 mm; Synthra Reeperbahn, Hamburg, Germany) at the UV wavelength of 254 nm. The HPLC loop volume was 5 mL and the mobile phase was a mixture of acetonitrile and 0.1% TFA in water (v/v = 40/60) at a flow rate of 6 mL/min. The retention time of [^{18}F]FMPEP-d_2 was about 15 min.

Analytical Acquity ultra-performance liquid chromatography (UPLC) system (Waters, Milford, MA, USA) equipped with ultraviolet (UV) and

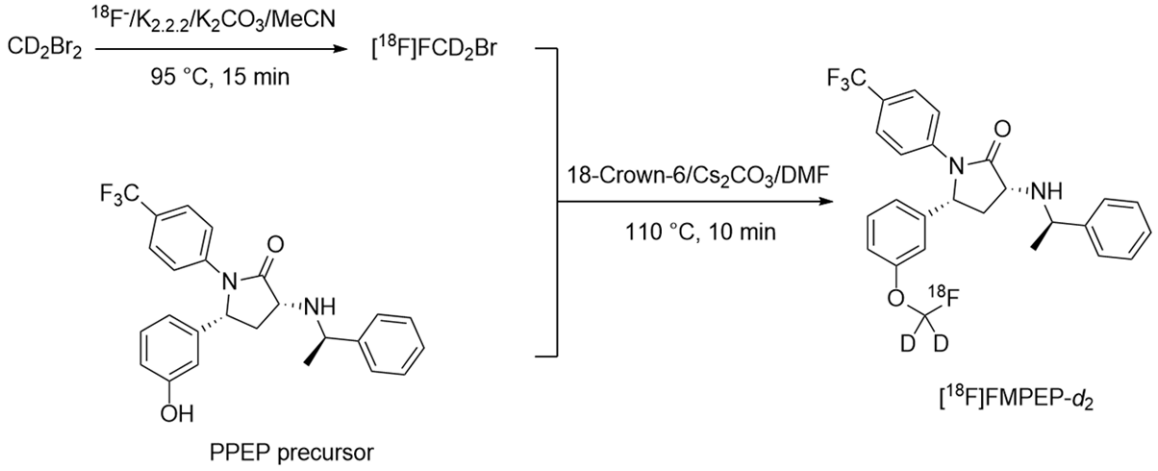

Figure 2. Radiosynthesis of [^{18}F]FMPEP-d_2.

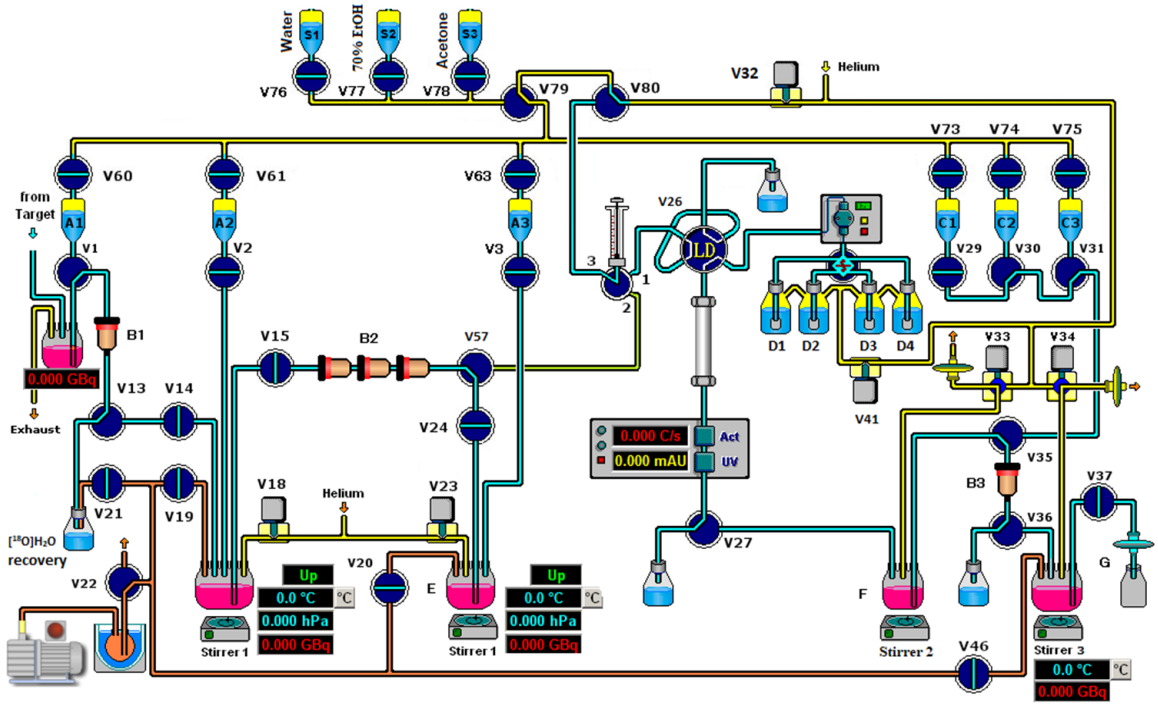

Figure 3. Diagram of Synthra RNplus research module for [^{18}F]FMPEP-d_2 production.

Ortec-556 radioactivity detectors (Oak Ridge, TN, USA) was used to determine radiochemical purities and identities, and chemical impurities on an analytical ACQUITY BEH C18 column (1.7 μm, 2.1 × 100 mm; Waters, Milford, MA, USA) at the UV wavelength of 254 nm. The sample injection volume was 10 μL and the mobile phase was a mixture of acetonitrile and 0.1% TFA in water (v/v = 45/55) with a flow rate of 0.3 mL/min. The retention time of [^{18}F] FMPEP-d_2 on analytical HPLC was about 3.6 min.

RNplus research module configuration

Synthra RNplus research module is a desirable automated synthesizer for F-18 radiotracers production. The module configuration and setup for [^{18}F]FMPEP-d_2 production were detailed in **Figure 3** and **Table 1**. In the optimized module configuration, vials A1-A3, C1-C3, Sep-Pak cartridges B1-B3, and reaction vessels 1 and 2 were used for [^{18}F]FMPEP-d_2 radiosynthesis followed by HPLC purification (**Figure 4**), solid phase extraction and formulation. Through

Table 1. Synthra RNplus module setup list for [^{18}F]FMPEP-d_2 production

Location	Items
A1	1 mL of $K_{2.2.2}/K_2CO_3$ solution
A2	100 μL of CD_2Br_2 and 0.8 mL of MeCN
A3	1 mL of water
B1	QMA cartridge (46 mg)
B2	three Silica Plus cartridges
B3	C18 plus cartridge
C1	10 mL of sterile water
C2	1 mL of ethanol
C3	1 mg ascorbic acid in 10 mL of 0.9% NaCl
D1	HPLC eluent: MeCN/0.1% TFA (v/v = 40/60)
E	0.5 mg precursor/5 mg 18-crown-6/0.5 mg Cs_2CO_3 in 0.5 mL DMF
F	30 mL of deionized water
G	30 mL product vial and vent Millex-LG filter

the shared valve V57, a needle in the reaction vessel-2 was allowed to transfer the gaseous [^{18}F]FCD_2Br intermediate into precursor solution with bubbling, and load the reaction mixture for HPLC purification after reaction.

Radiosynthesis, purification, and formulation of [^{18}F]FMPEP-d_2

By irradiation of [^{18}O]water with a GE PETtrace 800 cyclotron (60 min irradiation at 60 μA), [^{18}F]fluoride was generated and delivered to Synthra RNPlus Research module for [^{18}F]FMPEP-d_2 radiosynthesis. The received [^{18}F]fluoride was extracted with a QMA cartridge (46 mg) and eluted with 1.0 mL of Kryptofix 2.2.2 (12 mg, 32 μmol) and potassium carbonate (2 mg, 14 μmol) solution, and then dried by azeotropic evaporation at 70-100°C under a flow of helium and/or vacuum. The reaction vessel-1 containing dried [^{18}F]fluoride was cooled to 50°C, and added with CD_2Br_2 (100 μL) in acetonitrile (0.8 mL). The mixture was heated at 95°C for 15 minutes to form [^{18}F]FCD_2Br and then cooled to 40°C. Via three silica cartridges, volatile [^{18}F]FCD_2Br was swept to reaction vessel-2, bubbling into a mixture of PPEP precursor (0.5 mg, 1.1 μmol), 18-crown-6 (5 mg, 19 μmol) and Cs_2CO_3 (0.5 mg, 1.5 μmol) in DMF (0.5 mL), which was preloaded and cooled to 0°C. At the end of transfer, [^{18}F]FCD_2Br was allowed to react with precursor at 110°C for 10 min. The formed crude product was cooled to 50°C, diluted with 1 mL of water and loaded onto a semi-preparative HPLC (Synthra Reeperbahn C18, 5 μm, 250 × 10 mm; 40% MeCN in 0.1% TFA; 6 mL/min) for purification. The collected [^{18}F]FMPEP-d_2 product fraction was diluted with 30 mL water, enriched on a C18 Plus cartridge, washed with sterile water (10 mL), and eluted with ethanol (1 mL). The final product was formulated with 0.9% NaCl (10 mL) and ascorbic acid (1 mg), and then sent to a vented 30 mL product vial through a sterile Millex-LG syringe filter.

Quality control

A sample of ~0.5 mL was taken from the finished final product for QC tests following United States Pharmacopeia and GMP guidelines. The detailed QC procedure was described in Supplementary Materials.

Results and discussion

Radiosynthesis

[^{18}F]FMPEP-d_2 product were obtained in 2.2 ± 0.1 GBq (EOS) from estimated starting activity of 130 GBq in three consecutive validation runs. [^{18}F]FMPEP-d_2 radiosynthesis were completed in a total synthesis time of 70 min from EOB. The final product were formulated in volumes of 10.0 ± 0.2 mL containing 10 mL 0.9% NaCl, 6-8% ethanol and 1 mg of ascorbic acid as a stabilizer. The radiochemical yields were 2.5 ± 0.1% (decay corrected to EOB).

Quality control

The QC results showed that the produced [^{18}F]FMPEP-d_2 met all the release criteria for human use. As indicated in **Table 2**, all three batch products were clear, colorless solutions, and free from particulate matter. The pH and half-life values were within the ranges of 4.0-7.0 and 105-115 min. From analytical HPLC results (**Figure 5**), excellent radiochemical purities were achieved at > 99.9%. The nonradioactive mass of [^{18}F]FMPEP-d_2 were 0.08 ± 0.02 μg/mL and the total unknown impurities were 0.073 ± 0.005 μg/mL. The radionuclidic purities were determined by no observed long-lived isotopes existence in the product after decay. The resid-

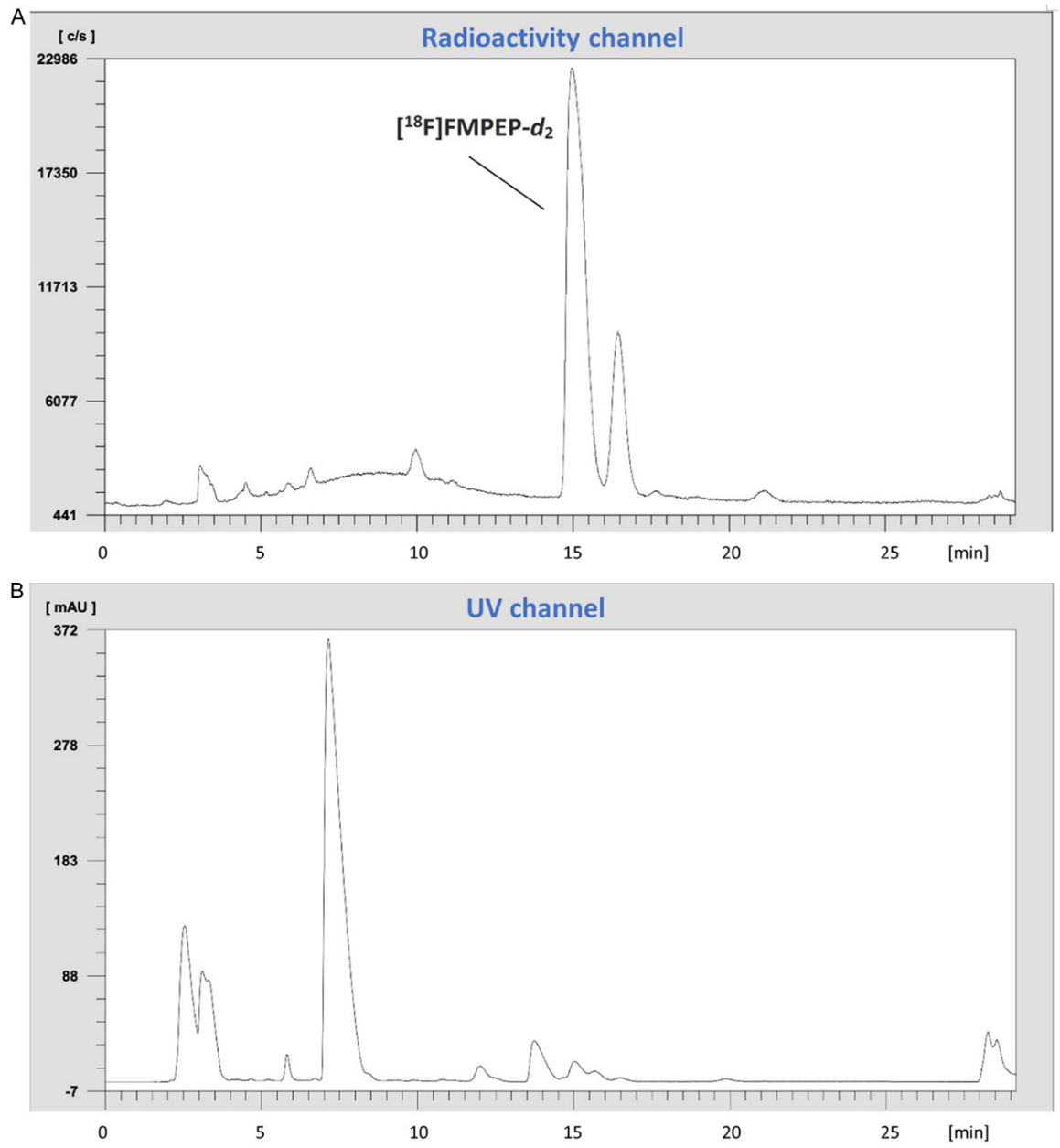

Figure 4. Representative semi-preparative HPLC chromatograms for [^{18}F]FMPEP-d_2 purification. (A) Radioactivity channel and (B) UV channel.

ual solvents in product were determined to be 6.7-8.0% ethanol. The integrity of the final filter was demonstrated by a bubble-point filter test with holding ≥ 45 psi pressure. The formulated products were sterile and nonpyrogenic from the sterility and endotoxin results. Stability at 4 hours after EOS was evaluated by performing the repeated assessment of appearance, radiochemical identity/purity, chemical purity, pH, and bacterial endotoxin. A summary of the stability tests was given in Table S1, showing no significant changes at 4 hours post EOS.

Discussion

With the starting activity 130 GBq from 60 min irradiation at 60 μA, [^{18}F]FMPEP-d_2 product were obtained in 2.2 ± 0.1 GBq, which was able to meet the needs of our clinical trials, typically a couple doses for each batch. The yield in this

Table 2. Summary of QC results from three [^{18}F]FMPEP-d_2 validation runs

QC Test	Acceptance Criteria	Result		
		Run 1	Run 2	Run 3
Appearance	Clean, colorless and no particles	Pass	Pass	Pass
Concentration	74-740 MBq/mL at EOS	218 MBq/mL	204 MBq/mL	241 MBq/mL
Filter integrity	Bubble point ≥ 45 psi	Pass	Pass	Pass
Radionuclidic identity	Half-life: 105-115 min	109.8 min	109.7 min	109.8 min
Radionuclidic purity	≥ 99.5% observed gamma emission should correspond to 0.511 and 1.022 MeV	Pass	Pass	Pass
pH	pH value: 4.0-7.0	5.0	5.0	5.0
Radiochemical purity	[^{18}F]FMPEP-d_2 peak: ≥ 90%	> 99%	> 99%	> 99%
Radiochemical identity	RSD of [^{18}F]FMPEP-d_2 Rt values: ≤ 10%	3.7%	3.4%	3.6%
Chemical purity	FMPEP mass: ≤ 2 μg/mL Impurity: ≤ 4 μg/mL	FMPEP: 0.06 μg/mL Impurity: 0.08 μg/mL	FMPEP: 0.10 μg/mL Impurity: 0.07 μg/mL	FMPEP: 0.09 μg/mL Impurity: 0.07 μg/mL
Chemical purity: residual solvent	Ethanol ≤ 10% (w/v)	8.0%	6.7%	6.8%
	MeCN ≤ 0.041% (w/v)	0%	0%	0%
	DMF ≤ 0.088% (w/v)	0%	0%	0%
Chemical purity: $K_{2.2.2}$	Intensity is less than $K_{2.2.2}$ STD	Pass	Pass	Pass
Pyrogen test	LAL endotoxins test: ≤ 175 EU/vial	Pass	Pass	Pass
Sterility test	No growth after 2 weeks incubation	Pass	Pass	Pass

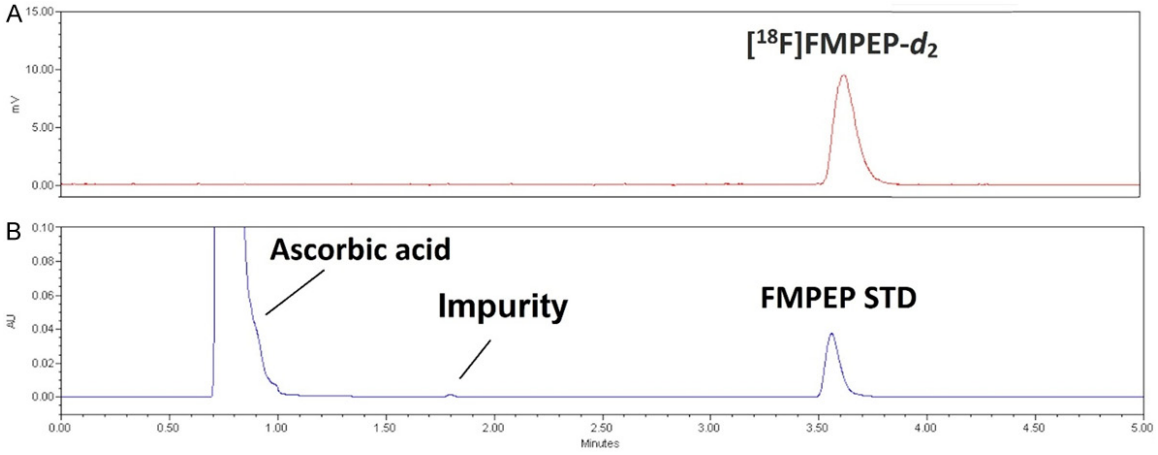

Figure 5. Representative analytical HPLC chromatograms of [^{18}F]FMPEP-d_2 and reference co-injection. (A) Radioactivity channel and (B) UV channel.

work (2.5 ± 0.1%) was lower than that of the reported method (7.93 ± 2.48%) [12]. It is difficult to make head-to-head comparisons with limited automation data published, but the difference may be caused by the following reasons. Firstly, the starting activity for yield calculation in this work was not calibrated at arrival of Synthra RNPlus module but obtained from the cyclotron bombardment report. Limited by the facility layout, the hot cell and module for [^{18}F]FMPEP-d_2 synthesis were located at over 60 meters away from the cyclotron, resulting in activity loss during [^{18}F]fluoride delivery. Secondly, the TRACERlab FX_{F-N} module used in the literature was modified to send gaseous [^{18}F]FCD_2Br at a slow flowrate (30 mL/min). In our synthesis, [^{18}F]FCD_2Br was swept directly at much higher flowrate, which may give reduced trapping efficiency when bubbling into 0.5 mL DMF solution. Lastly, in the literature, 9.5 mL of ethanol was used to elute [^{18}F]FMPEP-d_2 from the C18 plus cartridge for HPLC fraction extraction. Given to typically less than 10% ethanol concentration in PET drugs for in-human administration, only 1 mL of ethanol was used in our method and resulted in lower elution recovery. During the optimiztion, more precursor was tried but gave little improvement in the radiochemical yield (data not shown). The low radiochemical yield was also because of that the

formed [^{18}F]FCD_2Br in the reaction vessel 1 was not be completely swept to the precursor vessel. Lahdenpohja et al. [16] reported an improved [^{18}F]FMPEP-d_2 synthesis with decay-corrected yield of 16 ± 6%, by addition of a gas chromatography for [^{18}F]FCD_2Br separation on an in-house built module. However, their method requires extra 15 minutes for [^{18}F]FCD_2Br fraction collection, and time for gas chromatography conditioning and maintenance. Considering the limited space in the hotcell and simplicity of automation, we followed Donohue et al.'s method using three disposable silica cartridges for [^{18}F]FCD_2Br separation as trade-off of higher radiochemical yield.

A reliable formation and distillation of [^{18}F]FCD_2Br is the prerequisite for the successful [^{18}F]FMPEP-d_2 synthesis. To apply [^{18}F]FCD_2Br chemistry, RNplus module configuration was modified by sharing valve 57 for [^{18}F]FCD_2Br distillation and HPLC sample loading (**Figure 3**). At [^{18}F]FCD_2Br distillation step, the needle was able to be inserted at the bottom of reaction vessel 2, so that the volatile [^{18}F]FCD_2Br could be trapped in DMF solution through bubbling. To avoid the loss of [^{18}F]FCD_2Br during heating, leak check on reaction vessel 1 was performed with pressurized helium through valve 18, prior to each synthesis. During [^{18}F]FCD_2Br distillation through three silica cartridges, the received [^{18}F]FCD_2Br activity was monitored by the radioactive detector located beside reaction vessel 2. Once the activity curve reached to the plateau, the distillation was terminated immediately to reduce the breakthrough of CD_2Br_2.

During the method development, unknown radiochemical byproducts following [^{18}F]FMPEP-d_2 peak were found occasionally on semi-preparative HPLC chromatography (Figure S1). This is probably caused by the hygroscopic nature of Cs_2CO_3 and thereby decomposition of precursor, considering the timepoint variations of precursor/18-crown-6/Cs_2CO_3 mixing. To be consistent, Cs_2CO_3 was not weighted and mixed with precursor/18-crown-6 until 15 min before EOB for [^{18}F]FMPEP-d_2 routine production. As a result, the formation of such impurity peaks was largely inhibited (**Figure 4**).

It is worth mentioning that [^{18}F]FMPEP-d_2 is a lipophilic compound and thereby easily precipitated and sticks to plastic materials. When [^{18}F]FMPEP-d_2 dose was prepared and stored in a syringe and/or loop for 30 minutes, up to 80% activity was found sticking to syringe and extension loop. In our practice, [^{18}F]FMPEP-d_2 dose was prepared right away before injection, and avoided unnecessary dilution, and leftover activity in syringe and/or extension loop was measured and subtracted to get the corrected activity administrated.

Conclusions

A fully automated production of [^{18}F]FMPEP-d_2 was achieved in excellent radiochemical and chemical purity, and a reasonable radiochemical yield. Three consecutive [^{18}F]FMPEP-d_2 validation runs and quality control results demonstrated its efficacy for in-human CB1R PET imaging, which has been evaluated at Karmanos PET center under Radioactive Drug Research Committee (RDRC).

Acknowledgements

This work has been supported by Karmanos Cancer Institute and Wayne State University School of Medicine. The Cyclotron and Radiochemistry Core is supported, in part, by NIH Center grant P30 CA022453 to the Karmanos Cancer Institute at Wayne State University.

Disclosure of conflict of interest

None.

Address correspondence to: Huailei Jiang, Cyclotron and Radiochemistry Core, Karmanos Cancer Institute, Detroit, MI, USA. E-mail: jiangh@karmanos.org

References

[1] Cristino L, Bisogno T and Di Marzo V. Cannabinoids and the expanded endocannabinoid system in neurological disorders. Nat Rev Neurol 2020; 16: 9-29.

[2] Herkenham M, Lynn AB, Little MD, Johnson MR, Melvin LS, de Costa BR and Rice KC. Cannabinoid receptor localization in brain. Proc Natl Acad Sci U S A 1990; 87: 1932-6.

[3] Kruk-Slomka M, Dzik A, Budzynska B and Biala G. Endocannabinoid system: the direct and indirect involvement in the memory and learning processes-a short review. Mol Neurobiol 2017; 54: 8332-8347.

[4] Lutz B, Marsicano G, Maldonado R and Hillard CJ. The endocannabinoid system in guarding against fear, anxiety and stress. Nat Rev Neurosci 2015; 16: 705-18.

[5] Howlett AC, Blume LC and Dalton GD. CB(1) cannabinoid receptors and their associated proteins. Curr Med Chem 2010; 17: 1382-1393.
[6] Fernández-Ruiz J. The endocannabinoid system as a target for the treatment of motor dysfunction. Br J Pharmacol 2009; 156: 1029-40.
[7] Zhang L, Chang RC, Chu LW and Mak HK. Current neuroimaging techniques in Alzheimer's disease and applications in animal models. Am J Nucl Med Mol Imaging 2012; 2: 386-404.
[8] Morbelli S and Nobili F. Cognitive reserve and clinical expression of Alzheimer's disease: evidence and implications for brain PET imaging. Am J Nucl Med Mol Imaging 2014; 4: 239-47.
[9] Holland JP, Cumming P and Vasdev N. PET radiopharmaceuticals for probing enzymes in the brain. Am J Nucl Med Mol Imaging 2013; 3: 194-216.
[10] Charalambous A, Marciniak G, Shiue CY, Dewey SL, Schlyer DJ, Wolf AP and Makriyannis A. PET studies in the primate brain and biodistribution in mice using (-)-5'-18F-delta 8-THC. Pharmacol Biochem Behav 1991; 40: 503-7.
[11] Li Z, Gifford A, Liu Q, Thotapally R, Ding YS, Makriyannis A and Gatley SJ. Candidate PET radioligands for cannabinoid CB1 receptors: [18F]AM5144 and related pyrazole compounds. Nucl Med Biol 2005; 32: 361-6.
[12] Donohue SR, Krushinski JH, Pike VW, Chernet E, Phebus L, Chesterfield AK, Felder CC, Halldin C and Schaus JM. Synthesis, ex vivo evaluation, and radiolabeling of potent 1,5-diphenylpyrrolidin-2-one cannabinoid subtype-1 receptor ligands as candidates for in vivo imaging. J Med Chem 2008; 51: 5833-42.
[13] Borgan F, Laurikainen H, Veronese M, Marques TR, Haaparanta-Solin M, Solin O, Dahoun T, Rogdaki M, Salokangas RK, Karukivi M, Di Forti M, Turkheimer F, Hietala J and Howes O; METSY Group. In vivo availability of cannabinoid 1 receptor levels in patients with first-episode psychosis. JAMA Psychiatry 2019; 76: 1074-1084.
[14] Lahesmaa M, Eriksson O, Gnad T, Oikonen V, Bucci M, Hirvonen J, Koskensalo K, Teuho J, Niemi T, Taittonen M, Lahdenpohja S, U Din M, Haaparanta-Solin M, Pfeifer A, Virtanen KA and Nuutila P. Cannabinoid type 1 receptors are upregulated during acute activation of brown adipose tissue. Diabetes 2018; 67: 1226-1236.
[15] Hirvonen J, Zanotti-Fregonara P, Umhau JC, George DT, Rallis-Frutos D, Lyoo CH, Li CT, Hines CS, Sun H, Terry GE, Morse C, Zoghbi SS, Pike VW, Innis RB and Heilig M. Reduced cannabinoid CB1 receptor binding in alcohol dependence measured with positron emission tomography. Mol Psychiatry 2013; 18: 916-21.
[16] Lahdenpohja S, Keller T, Forsback S, Viljanen T, Kokkomäki E, Kivelä RV, Bergman J, Solin O and Kirjavainen AK. Automated GMP production and long-term experience in radiosynthesis of CB_1 tracer [^{18}F]FMPEP-d_2. J Labelled Comp Radiopharm 2020; 63: 408-418.
[17] Jiang H, Jain MK and Cai H. Automated production of [^{18}F]Flortaucipir for PET imaging of tauopathies. Am J Nucl Med Mol Imaging 2021; 11: 167-177.
[18] Jiang H, Guo Y, Cai H, Viola N, Shields AF, Muzik O and Juhasz C. Automated radiosynthesis of 1-(2-[^{18}F]fluoroethyl)-L-tryptophan ([^{18}F]FETrp) for positron emission tomography (PET) imaging of cancer in humans. J Labelled Comp Radiopharm 2023; 66: 180-188.
[19] Pereira MP, Tejería ME, Zeni M, Gambini JP, Duarte P, Rey A and Giglio J. Radiosynthesis and validation of [^{18}F]fluoroestradiol in a Synthra plus research platform for use in routine clinical practice. J Labelled Comp Radiopharm 2022; 65: 292-297.

Supplementary Materials

Detailed procedures for QC test

Appearance

Final product was visually observed through radiation shielding glass in adequate lighting to determine that the solution is clear, colorless, and free of particulates.

Radioactive concentration

The radioactivity of final product was measured with a dose calibrator. Assuming that the density of product is 1 g/mL, radioactive concentration of product was determined with the following equation:

Radioactive Concentration (mCi/mL) = $A/(W_1 - W_0)$.

A: activity of product.

W_0: weight empty vial.

W_1: weight of final product vial.

Filter Integrity

Followed by rinsing filter with 5 to 10 mL water, the integrity of the filter membrane was checked using the bubble point test.

Radionuclidic identity

Radionuclidic identity was determined by half-life ($t_{½}$). By placing a sample of drug product into a properly calibrated dose calibrator, record the activities at two time-points with a minimum of 10 minutes. $t_{½}$ was calculated by the following equation:

$t_{1/2}$ (min) = $(-0.693 * \Delta t)/(Ln(A_1) - Ln(A_0))$.

Δt (min): time difference between the first (t_0) and second (t_1) activity reading time point.

A_0 (mCi): first activity reading at t_0.

A_1 (mCi): second activity reading at t_1.

Radionuclidic purity

At the end of synthesis, measure the energy spectrum of product using a Multi-Channel Analyzer (MCA).

When F-18 in the product is decayed completely (e.g. 24-36 h), measure the same product sample with Multi-Channel Analyzer to detect the existence of long half-life radioisotopes in product, if any. F-18 radionuclidic purity was calculated with the areas of F-18 and other detected long half-life radioisotopes in product.

pH

A drop of product was placed onto a verified test strip covering the pH range of 2 to 9. pH value was visually checked on the color change and compared it to the pH color chart.

Chemical/radiochemical purity and identity

Chemical/radiochemical purity and identity were determined by analytical reverse phase C18 HPLC. The following parameters were used for the analysis.

HPLC conditions	Analytical C18 HPLC
Column	ACQUITY UPLC BEH C18, 1.7 μm, 100 × 2.1 mm
Eluent	Acetonitrile/0.1% TFA = 45/55 (V/V)
Flowrate	0.3 mL/min
UV	254 nm

(1) Load standard sample set and inject reference standard solution (10 μg/mL) onto HPLC column three times. Record retention times and peak areas of the three reference standard samples into the QC worksheet. The relative standard deviations (RSD) must be ≤ 10%.

(2) Inject a sample of final drug product, and record the retention times and peak areas from both the UV and Radiometric chromatograms into the QC worksheet to calculate radiochemical identity, radiochemical purity, and chemical purity.

(3) The radiochemical identity is determined by the following equation: % Shift = (|(Rt sample - Rt ref std)|/Rt ref std) *100.

(4) The radiochemical purity is the percent peak area reported in the radiometric chromatogram for the peak identified as the drug product.

(5) Chemical impurities from HPLC are evaluated through an analysis of the UV chromatogram of the drug product. All observable peaks (except peak of injection) are integrated. The peak areas are used to calculate the concentration of chemical impurities, assuming they have the same structure and molecular weight of reference standard.

Impurities concentration = (UV peak area of total impurities in drug product) * (conc of ref std)/(mean UV peak area of ref std).

Chemical purity - residual kryptofix ($K_{2.2.2}$)

(1) Place a drop of the 50 μg/mL $K_{2.2.2}$ standard solution (e.g. 1 μL) on a silica gel strip pretreated with iodoplatinate solution.

(2) Place a drop of the finalproduct solution (e.g. 1 μL; same volume as the $K_{2.2.2}$ standard) onto the strip, and compare the intensity of the two spots.

(3) A dark spot indicating the presence of $K_{2.2.2}$ will be observed for the $K_{2.2.2}$ reference solution. The spot of the final product must be negative or less intense than that of the $K_{2.2.2}$ reference solution.

Chemical purity - residual solvents

(1) Residual solvents were analyzed by an Agilent 7890A gas chromatograph (GC) system (Santa Clara, CA, USA) with a DB-WAX column (30 m × 0.53 mm × 1 μm). The injection volume was 0.5 μL. The GC method was holding at 40°C for 1 min after injection, and then increasing to 130°C with a rate of 20°C/min, and hold at 130°C for 1 min. the total run time is 6.5 min.

(2) Three replicates of GC standard solution (0.1% ethanol and 0.04% acetonitrile in water) were injected into the GC system, followed by a sample of 20-fold diluted final product solution (e.g. 25 μL product and 475 μL water).

(3) Using QC worksheet, the amount of residual solvents present in final product was calculated based on the integrated peak area obtained.

Pyrogen test - endotoxin

The pyrogen test was performed with an Endosafe-PTS device. Dilute the final product with sterile water (e.g. 1:50 dilution; 25 μL product and 1.25 mL sterile water), and then add 25 μL of the diluted product sample to each well of an Endosafe-PTS cassette. The total endotoxin limit for the undiluted product must be ≤ 175 EU/vial, considering the whole vial will be injected as a unit dose.

Sterility test

Within 30 hours after the completion of production, tryptic soy broth (TSB) and fluid thioglycollate (FTM) media tubes were directly inoculated with 0.1-1 mL of the decayed final product. The media tubes were observed with a minimum of three times (e.g. day 1-3, day 5-7 and day 14) after inoculation, for any microbial growth.

Stability test

The stability test was performed by second quality control tests (if applicable) of final product at four hours after EOS.

Table S1. Summary stability results at 4 hours after EOS of [^{18}F]FMPEP-d_2 validation runs

QC Test	Acceptance Criteria	Result		
		Run 1	Run 2	Run 3
Appearance	Clean, colorless and no particles	Pass	Pass	Pass
Radionuclidic identity	Half-life: 105-115 min	109.4 min	110.0 min	107.1 min
pH	pH value: 4.0-7.0	5.0	5.0	5.0
Radiochemical purity	[^{18}F]FMPEP peak: ≥ 90%	100%	100%	100%
Radiochemical identity	RSD of [^{18}F]FMPEP-d_2 Rt values: ≤ 10%	3.7%	3.3%	3.1%
Chemical purity	FMPEP mass: ≤ 2 μg/mL Impurity: ≤ 4 μg/mL	FMPEP: 0.02 μg/mL Impurity: 0.07 μg/mL	FMPEP: 0.12 μg/mL Impurity: 0.08 μg/mL	FMPEP: 0.13 μg/mL Impurity: 0.08 μg/mL
Chemical purity: $K_{2.2.2}$	Intensity is less than $K_{2.2.2}$ STD	Pass	Pass	Pass
Pyrogen test	LAL Endotoxins test: < 175 EU/vial	Pass	Pass	Pass

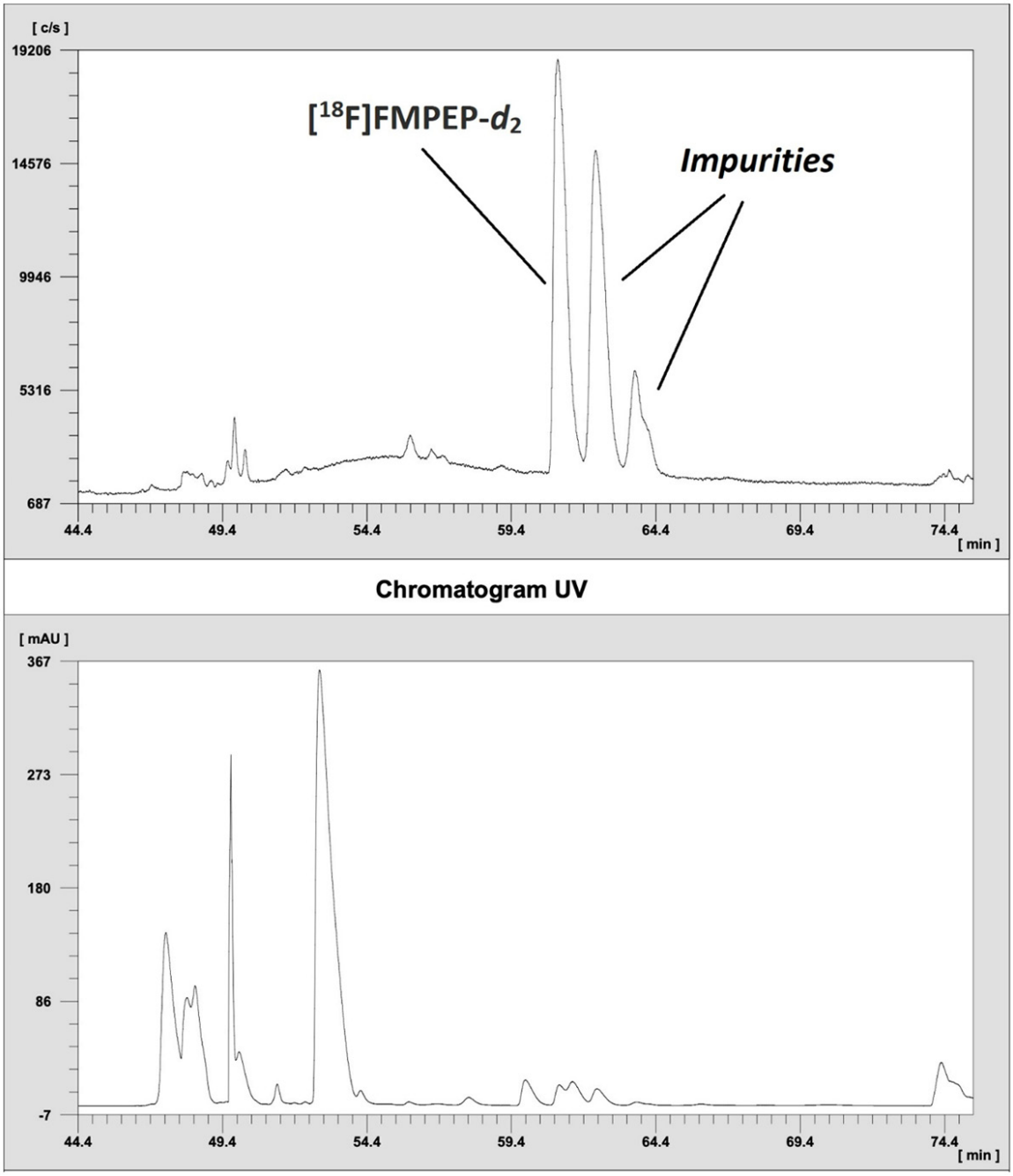

Figure S1. Impurities found during [^{18}F]FMPEP-d_2 semi-preparative separation.